are qualitatively correct, the strong association between chloride anions and a peptide would be expected for other zwitterions, or residues with positively charged side chains, and maybe even neutral peptide groups. If this so, the possible effects of the specific association of ions on peptide conformation will considerably complicate a number of present computationally convenient modeling techniques.

Timasheff and Arakawa have found that the salting-out of proteins can be decomposed into two contributions.[59] One from nonspecific preferential exclusion of the cosolvent from the protein surface and one from the specific binding of the ligand to the protein. The balance between these two effects leads to either solubilization or precipitation. Within the cations Na^+, Mg^{2+}, Ca^{2+}, Ba^{2+} and guanidinium, sodium had the highest preferential exclusion while for the anions Cl^-, AcO^-, and SO_4^{2-}, chloride ion was the least preferentially excluded.[59] This is certainly in agreement with the simulations described here. In addition, Arakawa and Timasheff also observed the binding of NaCl to β-lactoglobin and attributed this binding to the large dipole moment of the protein.[60] As chloride ions are the least preferentially excluded and sodium ions the most preferentially excluded from the protein surface,[59] this suggests binding of the chloride ions to β-lactoglobin. These observations are again in agreement with the above simulations.

From these simulations it is not possible to gain any real insight into the relative binding of other ions. This will only be possible by further simulations with different salts. However, in the case studied here the effects are dominated by anions with the cations acting as spectator ions.

Acknowledgment. We thank Prof. Victor J. Hruby, Dr. Fahad Al-Obeidi, and Dr. James M. Briggs for numerous interesting discussions and the Robert A. Welch Foundation and the National Institutes of Health for partial support. Finally we thank the San Diego Supercomputer Center for generous use of their Cray X-MP and Y-MP machines.

Appendix

The Ewald potential[31] for a system of N atoms each carrying a charge, q, in a box of length, L, surrounded by a medium of dielectric, ϵ', is given by[32]

$$V(r,\epsilon') = \sum_{1<i<j\le N} q_i q_j \psi(r_{ij}) + \frac{\xi}{2}\sum_{i=1}^{N} q_i^2 + \frac{2\pi}{(2\epsilon'+1)L^3}\left|\sum_{i=1}^{N} q_i \mathbf{r}_i\right|^2 \quad (1)$$

where

$$\psi(r) = \sum_{|\mathbf{n}|=0}^{\infty} \frac{\operatorname{erfc}(\kappa|\mathbf{r}+\mathbf{n}L|)}{|\mathbf{r}+\mathbf{n}L|} + \frac{1}{\pi L}\sum_{|\mathbf{n}|\neq 0}^{\infty}\frac{1}{|\mathbf{n}|^2}\exp\left(\frac{2\pi i}{L}\mathbf{n}\cdot\mathbf{r} - \frac{\pi^2|\mathbf{n}|^2}{\kappa^2 L^2}\right) \quad (2)$$

with

$$\xi = \sum_{|\mathbf{n}|\neq 0}^{\infty}\left[\frac{\operatorname{erfc}(\kappa|\mathbf{n}L|)}{|\mathbf{n}L|} + \frac{1}{\pi L|\mathbf{n}|^2}\exp\left(-\frac{\pi^2|\mathbf{n}|^2}{\kappa^2 L^2}\right)\right] - \frac{2\kappa}{\sqrt{\pi}} \quad (3)$$

and

$$\operatorname{erfc}(x) = 1 - \frac{2}{\sqrt{\pi}}\int_0^x \exp(-t^2)\,dt \quad (4)$$

The sum over the lattice vectors, $\mathbf{n}_x$, $\mathbf{n}_y$ and $\mathbf{n}_z$ is performed for all $|\mathbf{n}| \le 4$ which produces a spherical arrangement of 256 images around the central box. We used a value of $\kappa = 2.25/L$ with the so-called conducting, or "tin foil", boundary conditions ($\epsilon' = \infty$). Due to the computationally intensive nature of the Ewald sum a table lookup procedure was employed in our simulations. The Ewald potential, and its analytic first and second derivatives, were stored on a $50 \times 50 \times 50$ grid placed on the central box, and a cubic interpolation of the potential and a quartic interpolation of the force were then implemented to obtain the potential and force for a given interatomic separation.

Our simulations called for an infinitely dilute solution of DPDPE. This was achieved by skipping the interaction of DPDPE with its images in the surrounding periodic boxes. This results in the presence of a cavity in the periodic images. However, this did not seem to have any inadvertent effects on the dynamics of the system. As a check we performed a short finite concentration simulation of DPDPE by including the Ewald terms for all peptide–peptide image electrostatic interactions. There was no significant deviation in the structure or dynamics of the peptide or solvent from that obtained at infinite dilution.

Registry No. DPDPE, 88373-73-3; NaCl, 7647-14-5.

(57) Findsen, L. A.; Subramanian, S.; Pettitt, B. M. *Biophys. J.* Submitted for publication.
(58) Verrall, R. E. In *Water: A Comprehensive Treatise*; Franks, F., Ed.; Plenum Press: New York, 1973; Vol. 3, Chapter 5.
(59) Timasheff, S. N.; Arakawa, T. *J. Cryst. Growth* **1988**, *90*, 39-46.
(60) Arakawa, T.; Timasheff, S. N. *Biochemistry* **1987**, *26*, 5147-5153.

QCFF/PI Vibrational Frequencies of Some Spherical Carbon Clusters

Fabrizia Negri, Giorgio Orlandi, and Francesco Zerbetto*

Contribution from the Dipartimento di Chimica "G. Ciamician", Universita' di Bologna, Via F. Selmi 2, 40126 Bologna, Italy. *Received January 4, 1991*

Abstract: QCFF/PI calculations of the vibrational frequencies of C_{60}, C_{70}, and the two highest symmetry C_{84} carbon clusters are presented. The results should be of help in the assignment of the vibrational spectra of the newly isolated carbon clusters and possibly in determining the structure of C_{84}. The agreement between the calculated and the experimentally available frequencies is remarkable with the largest discrepancies of 30 cm^{-1} for C_{60} and 65 cm^{-1} for C_{70}. It is proposed that the QCFF/PI method be the method of choice to obtain the vibrational frequencies of fullerene molecules.

Introduction

Very recently the long quest for the C_{60} and C_{70} carbon clusters was met with success.[1] The two molecules were isolated and shown to have fullerene structure through the analysis of their NMR spectra.[2] Their full infrared, Raman, and UV characterization is now in progress.[3] It can be hoped that very soon

(1) Kratschmer, W.; Lamb, L. D.; Fostiropoulos, K.; Huffmann, D. R. *Nature* **1990**, *347*, 354-358.
(2) Taylor, R.; Hare, J. P.; Abdul-Sada, A. K.; Kroto, H. W. *J. Chem. Soc., Chem. Commun.* **1990**, 1423-1425.
(3) Bethune, D. S.; Meijer, G.; Tang, W. C.; Rosen, H. J. *Chem. Phys. Lett.* **1990**, *174*, 219-222.

0002-7863/91/1513-6037$02.50/0

Table I. Calculated and Experimental IR and Raman Active Frequencies of C_{60}

	a	b	c	d	e	f	exp[g]
h_g	1644	1830	1722		2068	1601	
	1465	1688	1596		1910	1468	
	1265	1398	1407		1575	1221	
	1154	1160	1261		1292	1004	
	801	780	924		828	743	
	691	552	771		526	645	
	440	428	447		413	435	
	258	272	263		274	218	273
t_{1u}	1437	1655	1628	1753	1868	1434	1429
	1212	1374	1353	1405	1462	1119	1183
	607	551	719	776	618	618	577
	544	491	577	574	478	472	528
a_g	1442	1627	1667	1798	1830	1409	1469
	513	548	610	660	510	388	497

[a] Reference 4. [b] Reference 8. Reference 9. [d] Reference 12. [e] Reference 10. [f] Reference 11. [g] References 1 and 3.

other compounds of this type will be isolated and that a thorough understanding of these molecules will be achieved.

Recently, we reported the vibrational frequencies of C_{60}[4] calculated by our upgraded QCFF/PI[5,6] method which has been of great help in our work on polyenic systems where it has been shown to be able to discriminate between different polyenic isomers.[6] At the time of our first report on C_{60}, no experimental data were available, and no comparison between experiment and computational theory was possible. The situation is now changed, and some frequencies have become available. The purpose of this work is 2-fold: on the one hand, we want to furnish a tool to assign the so far partially published spectrum of C_{70} and of the newly isolated C_{84}[7] for which two high symmetry structures (D_{6h} and T_d) are possible; on the other hand, we want to show that the QCFF/PI[5,6] method, once upgraded along the lines reported in ref 6f, is particularly effective in dealing with carbon clusters vibrational frequencies. The ability of QCFF/PI to handle these compounds should be of great help in the future for a number of reasons: (i) The synthesis of these molecules is obtained through a vaporization of graphite, and one is probably bound to collect a mixture of different compounds with rather similar molecular weights and possibly different isomers of the same weight. (ii) With very few exceptions, the point group symmetry of these molecules is lower than the I_h of C_{60}, so that the number of infrared or Raman active vibrations can be very large and change little from isomer to isomer. (iii) Semiempirical and ab initio quantum chemical methods are now routinely used to predict vibrational frequencies; however, for molecules of this size, they are very CPU intensive, and the vibrational frequencies calculated by them can easily be off the mark by 200–300 cm^{-1}.

Results and Discussion

In this section, we show that an upgraded QCFF/PI program furnishes a simple tool that can be used to predict the vibrational frequencies of carbon clusters. In general, sets of calculated frequencies may be used as fingerprints to identify these compounds either in the laboratory or, possibly, in the interstellar medium.

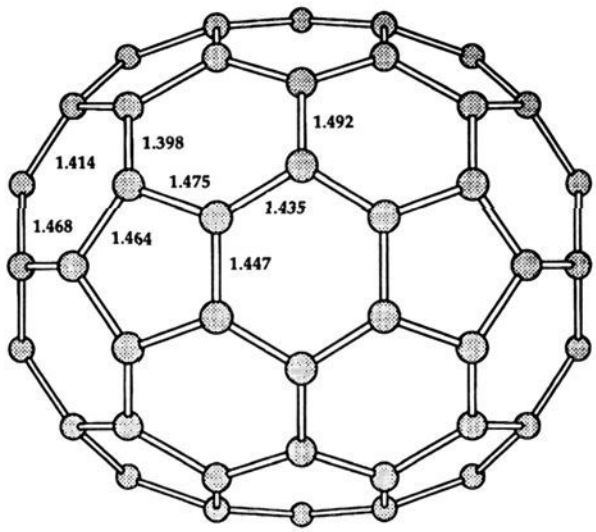

Figure 1. QCFF/PI optimized structure of C_{70}.

In the case of C_{84}, presented hereafter, if samples of the pure clusters (vide infra) are not available for NMR spectroscopy studies, they may also be used to determine the molecular structure.

In the following, structural information is also discussed.

C_{60} Cluster. In Table I, we report our previous prediction of the C_{60} infrared and Raman active frequencies together with other calculations and the corresponding experimental values. Given the high symmetry (I_h) of the C_{60} cluster, only four modes of t_{1u} symmetry are infrared active and 10 modes of a_g and h_g symmetry are Raman active. The small number of spectroscopically active vibrations allows an unambiguous comparison between calculated and observed frequencies. The agreement between the experiment and the QCFF/PI calculations shown in Table I is remarkable. The largest discrepancy is 30 cm^{-1}, and the difference between experimental and calculated frequencies is about 20 cm^{-1} on average. Further details of the results on C_{60} can be found in ref 4.

C_{70} Cluster. In Figure 1, we show the optimized structure of the C_{70} cluster. In agreement with the analysis of the NMR spectrum given in ref 2, this structure belongs to the D_{5h} point group.

Two radii define the intramolecular cavity in D_{5h} symmetry. The first radius along the C_5 axis is 4.03 Å; the second radius in the plane perpendicular to the C_5 axis is 3.60 Å. It is worth noticing that the longest bonds are calculated to be 1.492 Å, quite large a value for a bond between unsaturated carbon atoms. The shortest bond length is 1.398 Å, a value very similar to the carbon–carbon bond length in benzene.

Point group considerations show that the vibrational motions transform as

$$\Gamma_{vib} = 12a'_1(\text{Raman}) + 9a'_2 + 21e'_1(\text{IR}) + 22e'_2(\text{Raman}) + 12a''_1 + 9a''_2(\text{IR}) + 21e''_1(\text{Raman}) + 22e''_2$$

In Table II, we show all the calculated and the experimentally available vibrational frequencies of C_{70} determined through Raman spectroscopy. Because of the lack of detailed experimental data, the vibrational assignment is not straightforward, and the results of our calculations may be of help in further experimental work. The strong bands at 1568, 1232, 1185, and 1062 cm^{-1} are highly depolarized and can probably be assigned to totally symmetric vibrations. For the remaining bands, the depolarization ratio was not given, and the assignment can only be made on the basis of frequency match. An assignment is proposed in Table II according to which the largest (although still reasonably small) disagreement is found for the highest frequency mode (65 cm^{-1}). Two explanations are possible: either the mode is of e symmetry (notice that this would be at odds with the depolarization ratio of this

(4) Negri, F.; Orlandi, G.; Zerbetto, F. *Chem. Phys. Lett.* **1988**, *144*, 31–37.
(5) Warshel, A.; Karplus, M. *J. Am. Chem. Soc.* **1972**, *94*, 5612–5625. Warshel, A.; Levitt, M. QCPE 247, Indiana University, 1974.
(6) (a) Orlandi, G.; Zerbetto, F. *Chem. Phys.* **1986**, *108*, 187–195. (b) Zerbetto, F.; Zgierski, M. Z.; Orlandi, G.; Marconi, G. *J. Chem. Phys.* **1987**, *87*, 2505–2512. (c) Zerbetto, F.; Zgierski, M. Z.; Orlandi, G. *Chem. Phys. Lett.* **1987**, *141*, 138–142. (d) Zerbetto, F.; Zgierski, M. Z. *Chem. Phys. Lett.* **1988**, *143*, 153–162. (e) Zerbetto, F.; Zgierski, M. Z. *Chem. Phys. Lett.* **1988**, *144*, 437–444. (f) Zerbetto, F.; Zgierski, M. Z.; Negri, F.; Orlandi, G. *J. Chem. Phys.* **1988**, *89*, 3681–3688. (g) Zerbetto, F.; Zgierski, M. Z. *Chem. Phys. Lett.* **1988**, *151*, 526–530. (h) Zerbetto, F.; Zgierski, M. Z. *Chem. Phys. Lett.* **1989**, *157*, 515–520. (i) Negri, F.; Orlandi, G.; Zerbetto, F.; Zgierski, M. Z. *J. Chem. Phys.* **1989**, *91*, 6215–6224. (j) Drew, J.; Zerbetto, F.; Szabo, A. G.; Morand, P. *J. Phys. Chem.* **1990**, *94*, 4439–4446. (k) Zerbetto, F.; Zgierski, M. Z. *J. Chem. Phys.* **1990**, *93*, 1235–1245.
(7) Arbogast, J. W.; Darmanyan, A. P.; Foote, C. S.; Rubin, Y.; Diederich, F. N.; Alvarez, M. M.; Anz, S. J.; Whetten, R. L. *J. Phys. Chem.* **1991**, *95*, 11–12.

Table II. Calculated QCFF/PI Vibrational Frequencies of C_{70}

a'_1[a]	a'_2	e'_1[b]	e'_2[a]	a''_1	a''_2[b]	e''_1[a]	e''_2	exp[c]
1633	1532	1640	1645	1658	1565	1647	1642	1568 (a'_1)
1465	1452	1568	1583	1454	1389	1592	1551	
1383	1298	1499	1526	1342	1270	1461	1531	1513 (e'_2)
1220	1146	1424	1463	1041	1217	1440	1460	1232 (a'_1)
1187	859	1383	1433	899	1168	1360	1418	1185 (a'_1)
1085	828	1369	1332	774	895	1317	1358	1062 (a'_1)
732	653	1245	1265	722	684	1232	1245	
682	568	1200	1212	544	592	1186	1141	
570	484	1118	1064	335	485	1069	1107	571 (a'_1 or e'_2)
474		961	966		326	909	939	
404		931	868			806	867	
251		819	822			766	819	260 (a'_1 or e''_1)
		748	781			753	739	
		711	773			699	710	
		650	756			559	682	
		585	722			538	610	
		560	667			489	515	
		498	570			419	405	
		412	501			243	391	
		361	425				314	
		327	305					
			216					

[a] Raman active. [b] Infrared active. [c] Raman data from ref 3.

Table III. Calculated QCFF/PI Vibrational Frequencies of C_{84} (D_{6h} Symmetry)

a_{1g}[a]	a_{2g}	b_{1g}	b_{2g}	e_{1g}[a]	e_{2g}[a]	a_{1u}	a_{2u}[b]	b_{1u}	b_{2u}	e_{1u}[b]	e_{2u}
1685	1531	1596	1611	1663	1681	1646	1631	1628	1605	1684	1670
1499	1461	1497	1502	1608	1594	1483	1319	1463	1576	1573	1571
1316	1307	1445	1337	1491	1513	1331	1263	1359	1423	1488	1515
1212	1141	1328	1137	1419	1480	1036	1252	1301	1214	1438	1464
1197	852	1060	1046	1330	1422	897	1136	1104	933	1384	1421
1053	826	896	769	1290	1352	768	858	837	909	1361	1348
682	646	826	677	1255	1254	717	676	764	826	1241	1242
666	574	722	512	1191	1245	547	506	664	769	1175	1179
566	509	536	366	1032	1067	342	461	460	685	1146	1132
438		480		923	1019		280	298	663	990	896
365		346		826	847				444	896	873
204				754	808				293	819	790
				722	805					734	707
				695	771					708	697
				530	701					643	660
				527	686					583	647
				502	627					532	468
				372	511					468	431
				207	505					445	319
					377					352	280
					369					283	
					221						

[a] Raman active. [b] Infrared active.

band) or the self-consistent field level of electronic theory does not fully account for the π system interactions, a case that we have met before for polyenes.[6] Also notice that even if this band is assigned to a totally symmetric vibration, the average deviation between the calculated and the experimentally availably frequencies is smaller than 20 cm^{-1}.

C_{84} Clusters. We can now try to use the upgraded QCFF/PI method to obtain some information on systems for which even scantier data are available, namely the C_{84} cluster. The choice of this cluster is dictated by two considerations: First, in ref 7 it was mentioned that a C_{84} cluster has been isolated, and its characterization is now probably in progress. Second, in their thorough discussion of elemental carbon cages, Schmalz, Seitz, Klein, and Hite[13] proposed two highly symmetry electronically closed shell structures for this cluster, namely a D_{6h} and a T_d cluster. The same structures were also proposed in ref 14.

In the following, we have considered both structures. In the optimized structures (see Figure 2a,b), the longest bonds were 1.483 and 1.495 Å for T_d and the D_{6h} structures, respectively; the shortest were 1.365 and 1.375 Å. The radius of the intramolecular cavity of the cluster of T_d symmetry resulted in 3.71 Å. In analogy with the case of C_{70}, two radii define the cavity of the D_{6h} cluster. These were found to be 4.31 Å for the one in the plane perpendicular to the C_6 axis and 3.61 Å for the one along the C_6 axis. The cavity of the C_{84} cluster of D_{6h} symmetry is thus the largest among the clusters studied here, a feature that can possibly make this cluster an excellent host.

The D_{6h} configuration was found to be more stable than the T_d one of 23.6 kcal/mol. Due to the large amounts of energy involved in the preparation of these clusters and the relatively small energy difference between the two isomers, we believe that only a spectroscopic analysis can successfully assign the molecular symmetry. If samples of pure C_{84} are available, NMR spectroscopy is then the best suited technique to determine the mo-

(8) Wu, Z. C.; Jelski, D. A.; George, T. F. *Chem. Phys. Lett.* **1987**, *137*, 291–294.
(9) Stanton, R. E.; Newton, M. D. *J. Phys. Chem.* **1988**, *92*, 2141–2145.
(10) Weeks, D. E.; Harter, W. G. *Chem. Phys. Lett.* **1988**, *144*, 366–372.
(11) Cyvin, S. J.; Brendsdal, E.; Cyvin, B. N.; Brunvoll, J. *Chem. Phys. Lett.* **1988**, *143*, 377–380.
(12) Slanina, Z.; Rudzinski, M. J.; Togasi, M.; Osawa, E. *J. Mol. Struct. THEOCHEM* **1989**, *202*, 169–176.
(13) Schmalz, T. G.; Seitz, W. A.; Klein, D. J.; Hite, G. E. *J. Am. Chem. soc.* **1988**, *110*, 1113–1127.
(14) Fowler, P. W.; Cremona, J. E.; Steer, J. I. *Theor. Chim. Acta* **1988**, *73*, 1–26.

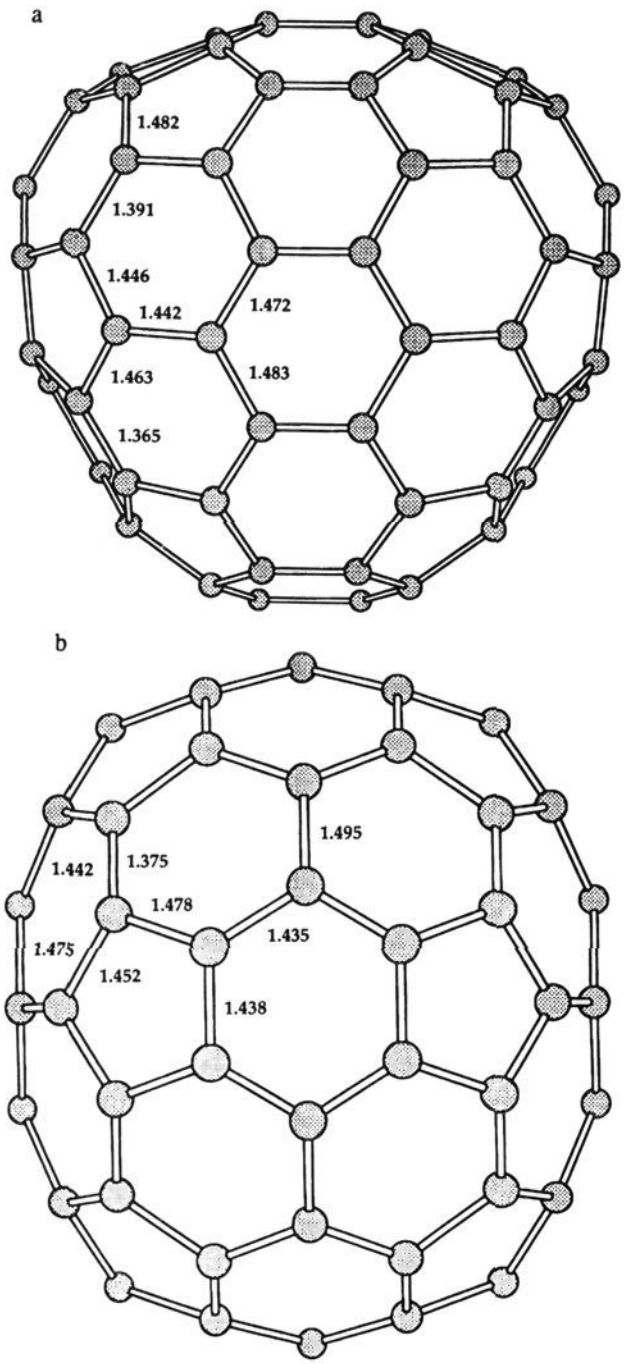

Figure 2. (a) *QCFF/PI* optimized structure of C_{84} T_d symmetry and (b) QCFF/PI optimized structure of C_{84} D_{6h} symmetry.

lecular structure. Otherwise, vibrational spectroscopy can be of help if one has ways of obtaining independent theoretical information, as it may be provided by the QCFF/PI program.

Point group theory shows that the vibrational modes of the two clusters transform as follows:

$$\Gamma_{vib}(D_{6h}) = 12a_{1g}(\text{Raman}) + 9a_{2g} + 11b_{1g} + 9b_{2g} + 19e_{1g}(\text{Raman}) + 22e_{2g}(\text{Raman}) + 9a_{1u} + 10a_{2u}(\text{IR}) + 10b_{1u} + 12b_{2u} + 21e_{1u}(\text{IR}) + 20e_{2u}$$

$$\Gamma_{vib}(T_d) = 11a_1(\text{Raman}) + 10a_2 + 21e(\text{Raman}) + 30t_1 + 31t_2(\text{IR, Raman})$$

Table IV. Calculated QCFF/PI Vibrational Frequencies of C_{84} (T_d Symmetry)

a_1[a]	a_2	e[a]	t_1	t_2[a,b]
1662	1603	1705	1665	1698
1517	1505	1664	1593	1624
1310	1416	1537	1554	1571
1289	1195	1456	1503	1490
1159	923	1431	1468	1471
1043	829	1396	1465	1430
850	774	1256	1395	1350
678	697	1231	1366	1329
435	549	1161	1316	1301
365	488	1061	1256	1248
294		860	1178	1219
		771	1044	1193
		721	999	1134
		697	917	1107
		663	902	1027
		650	856	885
		500	837	806
		449	829	795
		385	805	738
		329	745	709
		211	703	684
			697	674
			671	628
			574	541
			533	537
			513	497
			452	468
			366	440
			326	375
			289	286
				210

[a] Raman active. [b] Infrared active.

In Tables III and IV, we show the calculated vibrational frequencies for the two high symmetry C_{84} clusters. If we assume that for these two molecules, the QCFF/PI method has the same accuracy it shows for the experimentally available frequencies of the smaller clusters, one can easily find possible ways of distinguishing between the two compounds. By inspection of the two tables, good fingerprints can be furnished by the Raman active totally symmetric vibrations in the 1100–700-cm^{-1} region and by the infrared active modes below 300 cm^{-1}. In the first region, the T_d cluster has the first intervening mode of a_{1g} symmetry 193 cm^{-1} below the 1053-cm^{-1} mode. This gap is almost twice as large (371 cm^{-1}) for the cluster of D_{6h} symmetry. Although Raman active nontotally symmetric modes can be found in the 1100–700-cm^{-1} region for the D_{6h} cluster, these modes should not cause any problem in the spectral assignment if the depolarization ratios are available.

A second possible way of distinguishing between the two clusters is below the 300-cm^{-1} region. In this region, the lowest infrared active frequencies are 280 and 210 cm^{-1} for the D_{6h} and the T_d cluster, respectively. If the newly isolated cluster shows an infrared band in the 200-cm^{-1} region, this can be taken as a sign of the presence of the T_d cluster.

In this contribution, we have shown that the upgraded QCFF/PI method accounts very well for the experimentally available vibrational frequencies of fullerene molecules. On the basis of this result, we have predicted the remaining frequencies of C_{70} and of two high symmetry C_{84} isomers. Since there is no particular reason to think that the Raman and infrared active frequencies of C_{60} and C_{70} are calculated better than the nonactive ones or those of other carbon clusters, we suggest that the QCFF/PI quantum chemical method is an effective and powerful tool to calculate the vibrational frequencies of clusters of carbon atoms whose hybridization is close to sp^2.